

V. I. Dybkov, V. R. Sidorko,
V. G. Khoruzha, A. V. Samelyuk, L. V. Goncharuk
**INTERACTION OF 25% CHROMIUM STEEL
WITH BORON POWDER**

В результаті термохімічної обробки промислової хромової сталі (15X25T–25% Cr) в порошку аморфного бору в температурному інтервалі 850–950 °C і часі реакції до 43200 с (12 год) на межі розділу сталь–бор утворюються два боридних шари. Мікроструктура зовнішнього боридного шару, що межує з бором, складається з видовжених кристалів сполук (Fe, Cr)B і (Cr, Fe)B, а мікроструктура внутрішнього боридного шару, що прилягає до сталеві основи, складається з видовжених кристалів сполук (Fe, Cr)₂B і (Cr, Fe)₂B. Для обох шарів характерна яскраво виражена текстура. Кінетика їх дифузійного росту близька до параболічної $x^2 = 2k_1t$, де x — загальна товщина обох шарів (м), k_1 — константа швидкості росту шарів ($\text{м} \cdot \text{с}^{-1}$) і t — час (с). Температурна залежність константи швидкості росту боридних шарів на поверхні сталі описується залежністю Арреніусівського типу $k_1 = 1,72 \cdot 10^{-8} \exp(-137,1 \text{ кДж} \times \text{моль}^{-1}/RT)$. Величина мікротвердості становить 17,8 ГПа для зовнішнього шару, 15,9 ГПа для внутрішнього шару і 1,70 ГПа — для сталеві основи. Суха абразивна зносостійкість борованих зразків сталі більше, ніж у 250 разів вища зносостійкості неборованих зразків.

Ключові слова: термохімічна обробка, хромові сталь (15X25T–25% Cr), порошок аморфного бору, боридні шари, мікроструктура, кінетика росту, мікротвердість, абразивна зносостійкість.

Introduction

Boriding is one of the thermochemical surface treatments often used to improve service characteristics (hardness, wear resistance, etc.) of metals, alloys, and steels [1–4]. No ternary compounds are known to exist in the Fe–Cr–B system, whereas in appropriate binary systems there are two iron borides FeB and Fe₂B and seven chromium borides CrB₄, CrB₂, Cr₂B₃, Cr₃B₄, CrB, Cr₅B₃, and Cr₂B [5–8]. This work presents data on the microstructure, growth kinetics, and dry abrasive wear resistance of boride phases formed at the interface of industrial 25% chromium steel (15X25T) with amorphous boron powder in the temperature range 850–950°C.

Experimental Procedure

Materials and Specimens. The materials used included steel rods 16 mm in diameter, amorphous boron powder, and analytical-grade KBF₄. Initially, the boron powder contained 98.3% B, 0.04% C, 1.6% O, and insignificant amounts of Si, Cu, Mg (<0.01% each), and Fe (<0.001%). Before the boriding experiments, the powder was first heated slowly in vacuum up to 1450 °C and then calcined at this temperature for 2 h in an argon atmosphere at a pressure of $2.5 \times$

Table 1

Chemical Composition of Industrial 25% Chromium Steel (15X25T)

Method	C	Fe	Cr	Si	Mn	Ni	Ti
Certificate	0.13	72.8	25.2	0.46	0.50	0.45	0.28
CA	0.15	71.7	25.3	0.42	0.44	0.50	0.26
EPMA	—	72.4	25.1	0.49	0.48	0.43	0.29

Note: CA — chemical analysis, EPMA — electron probe microanalysis.

$\times 10^4$ Pa to remove volatile oxides. KBF_4 was preliminary dried in steps at 95, 110, 130, and 170 °C (24 h at each temperature).

The chemical composition of the steel is provided in Table 1. All contents are given in mass percent if otherwise not stated.

Specimens in the form of tablets, 11.28 mm in diameter (1.0 cm² area) and 5.5 mm in height, were machined from cylindrical steel rods. Flat sides of the tablets were ground and polished mechanically.

Experimental Methods. The VPBD-2S vacuum device employed for boriding steel samples has been described elsewhere [9]. Its experimental cell is shown in Fig. 1. The experiment was carried out in an alumina crucible, 13 mm in inner diameter and 40 mm high.

A steel tablet was embedded into a mixture of boron powder with 5% KBF_4 as an activator. This amount of KBF_4 is considered to be optimum [1, 10]. The mixture was then slightly pressed, and a load of 8.5 g (a low-carbon steel cylinder) was placed on top. The crucible was closed with a low-carbon steel lid and placed into a steel-sheet holder, mounted to a guide rod capable of moving in the vertical direction.

The chamber was pumped to a pressure of about 10 Pa and filled with high-purity argon (99.999 vol.% Ar). This procedure was repeated twice. Then, the chamber was again pumped and filled with argon at a pressure of 2.5×10^4 Pa, and heating was started. During heating, the crucible with its contents was in the cold zone above the furnace. After the required temperature in the range of 850–950 °C had been reached in the furnace, the crucible, pre-heated to about

400 °C, was moved into its middle part. After an initial drop, the temperature attained its pre-determined value in 4–5 min and was then maintained constant within ± 1 °C with the help of a VRT-3 automatic thermoregulator. The temperature measurements were carried out using a Pt–PtRh thermocouple. The experiments were carried out at temperatures of 850, 900, and 950 °C. Their duration was 3600–43200 sec (1–12 h).

After the experiment, the tablet with boride layers was cut along the cylindrical axis into two unequal

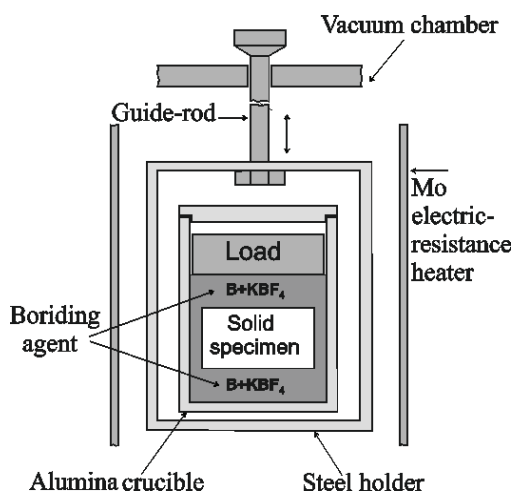


Fig. 1. Experimental cell

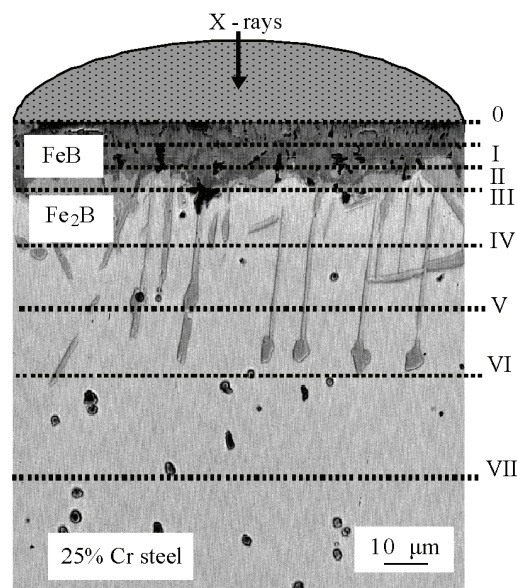


Fig. 2. Scheme of X-ray diffraction investigations of a borided 25% Cr steel sample:

boriding conditions: 950 °C, 21600 sec (6 h); the distance between successive sections of the sample (from top deeper inside its bulk) — 10 μm (0–I), 10 μm (I–II), 10 μm (II–III), 20 μm (III–IV), 20 μm (IV–V), 20 μm (V–VI), and 30 μm (VI–VII)

parts (4 and 7 mm) using an electric-spark machine. Its greater part was embedded into a cold-setting epoxy resin and used to prepare a metallographic cross-section. The smaller part was used for X-ray diffraction investigations (plan-view samples).

Characterization of boride layers was carried out with the help of metallography, X-ray diffraction (XRD), chemical analysis, and electron probe microanalysis (JEOL Superprobe 733 microanalyzer).

Table 2

Fe, Cr, and B Content of Reacting Phases, Found by EPMA on Borided Steel Samples after X-Ray Investigations (see also Figs. 2 and 4)

Section (see Fig. 2)	Region	Content (mass%/at.%)			Phase
		Fe	Cr	B	
I	Brighter in the outer boride layer (Fig. 4, a)	71.4/42.2	12.2/7.7	16.4/50.1	(Fe, Cr)B
	Darker in the outer boride layer (Fig. 4, a)	53.8/31.8	30.2/19.1	16.1/49.1	(Fe, Cr)B
II	Brighter in the outer boride layer (Fig. 4, b)	54.3/31.6	28.9/18.1	16.8/50.3	(Fe, Cr)B
	Darker in the outer boride layer (Fig. 4, b)	21.9/12.6	61.6/38.2	16.5/49.2	(Cr, Fe)B
III	Brighter in the inner boride layer (Fig. 4, c)	68.1/48.6	22.6/17.3	9.3/34.1	(Fe, Cr) ₂ B
	Darker in the inner boride layer (Fig. 4, c)	24.6/17.4	66.8/51.0	8.6/31.6	(Cr, Fe) ₂ B
IV	Bright in Fig. 4, d	84.1/83.2	15.9/16.8	0.0/0.0	<Fe>
	Dark in Fig. 4, d	27.0/18.8	63.8/48.0	9.2/33.2	(Cr, Fe) ₂ B
V	Bright	81.3/80.2	18.7/19.8	0.0/0.0	<Fe>
	Dark	24.6/17.4	66.8/51.0	8.6/31.6	(Cr, Fe) ₂ B
VI	One-phase	80.7/79.6	19.3/20.4	0.0/0.0	<Fe>

Fig. 3. Backscattered electron image (BEI) of the steel–boron transition zone and X-ray maps of iron and chromium:

the brighter a given region, the greater is the content of an appropriate component; boriding conditions: 950 °C, 25200 sec (7 h)

X-ray diffraction patterns were taken immediately from the surface of tablet samples on a DRON-3 apparatus using $\text{Cu-K}\alpha$ radiation. When taking the first pattern, no polishing of a borided sample was applied (section 0, Fig. 2). Then, 10 μm of a boride layer was removed by grinding and subsequent polishing, and another X-ray diffraction pattern was taken (section I). This procedure was repeated at a step of 10–30 μm until the steel base was reached (sections II–VII). Seven X-ray diffraction patterns were thus taken on each borided sample.

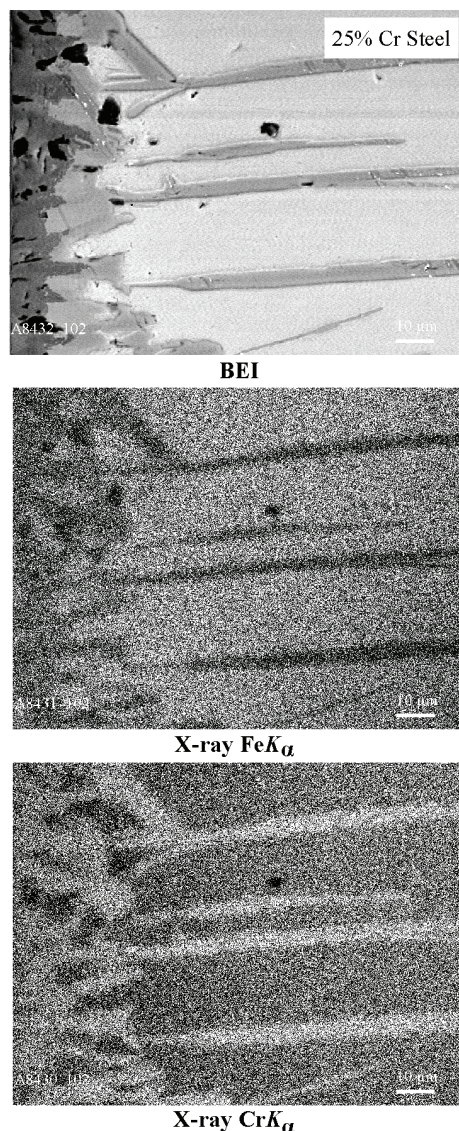
Microhardness measurements on metallographic cross-sections were carried out using a standard PMT-3 tester with a diamond pyramid (Vickers indenter). The load was 0.98 N (100 g).

Abrasive wear resistance tests (each along a fresh track) were carried out in the sliding mode on moving P180 SiC emery paper tape (main fraction grain size 63 μm , maximum 90 μm) using an AWRD-5 device [11]. The velocity of continuous movement of the tape (25.0 m long) was $0.35 \text{ m} \cdot \text{sec}^{-1}$, while the gauge length during each test was 22.0 m. The load was 50 N (5.1 kg). The wear resistance was determined by weighing the samples and measuring their height.

Phase Identity and Chemical Composition of Boride Layers

Two boride layers were found to form at the steel–boron interface (Figs. 2 and 3). Plan-view layer-by-layer X-ray analysis of borided samples and a further comparison of our and literature [12–16] data showed the outer layer bordering the boriding agent to be the FeB phase, while the inner layer adjacent to the alloy base to be the Fe_2B phase.

As seen from cross-sectional micrographs in Figs. 2 and 3, both layers consist of columnar crystals oriented preferentially in the direction of diffusion. Their characteristic feature is a tooth-like morphology and pronounced texture. This is considered to be a consequence of the paths of enhanced diffusion in the



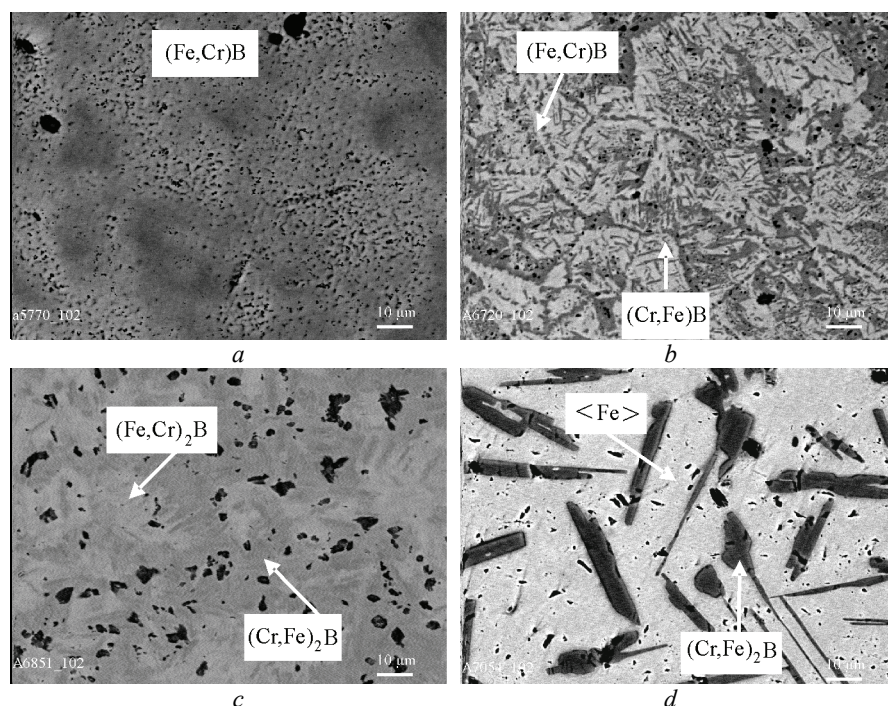


Fig. 4. Plan-view micrographs (BEI) corresponding to sections I–IV of a borided steel sample (see also Fig. 2)

crystal lattices of FeB and Fe₂B [1, 17]. If such paths are not available (close rates of diffusion in all crystallographic directions), flat boride layers are formed (see, for example, [10]).

The strongest reflections are {002} (experimental values: $2\theta = 63.3^\circ$ and spacing, $d = 0.1469$ nm) and, to a lesser extent, {020} ($2\theta = 32.6^\circ$ and $d = 0.2746$ nm) for the orthorhombic FeB phase, and {002} ($2\theta = 42.8^\circ$ and $d = 0.2113$ nm) for the tetragonal Fe₂B phase. Note that with isotropic microcrystalline samples the strongest reflections are {111}, {200}, and {210} for FeB and {211} for Fe₂B [12–16].

The larger orientation order is characteristic of the inner portions of both boride layers compared to their near-interface portions, in agreement with findings of other researchers [1, 17]. This is easily explainable because near-interface portions of any boride layer are less equilibrated compared to its inner portions. Therefore, near-interface crystals have less time to align in the preferred direction.

X-ray investigations were followed by EPMA measurements. Appropriate plan-view micrographs are shown in Fig. 4. Sections 0, I (Fig. 4, a) and II (Fig. 4, b) of a borided steel sample corresponded to a mixture of crystals of the FeB and CrB phases. Even though the CrB phase is not found by X-ray diffraction (perhaps, because its crystal structure is very similar to that of FeB [12–16] (especially if formed under highly non-equilibrium conditions, as in the present investigation), it can readily be revealed metallographically and by EPMA. Average Fe, Cr, and B contents of these and other phases are provided in Table 2.

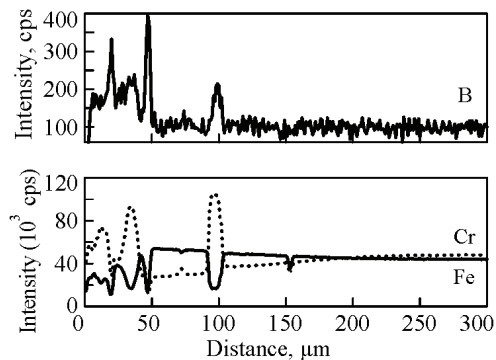
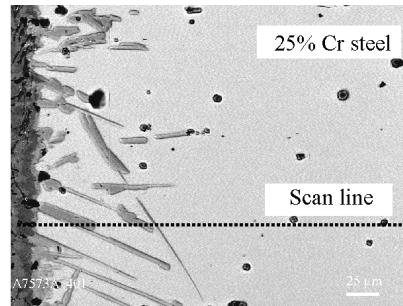
The dominant phase of section I is (Fe,Cr)B. The chromium content of its brighter regions is 7–12 at.%, whereas that of the darker ones is up to 20 at.%.

Fig. 5. Microstructure of the transition zone between 25% Cr steel and boron, and concentration profiles of boron, iron, and chromium:

boriding conditions: 950 °C, reaction time 21600 sec (6 h)

Black inclusions are borocarbides. In section II, the FeB and CrB phases are present in approximately equal amounts. Section III crossed both the FeB and Fe₂B phases (Fig. 4, c). Section IV corresponded to a solid solution of chromium in iron <Fe> and the (Cr, Fe)₂B phase. The microstructure of section V is similar to that of section IV, with the amount of the (Cr, Fe)₂B phase being much less. Section VI was the steel base, somewhat depleted in chromium, whereas section VII was entirely the steel base of nominal composition.

The distribution of chromium within the boride layers is rather irregular since both are in fact two-phase (Fig. 5). Wherever the iron content increases, the iron content is seen to decrease, and vice versa.



Microhardness of Boride Phases

Microhardness of the outer boride layer was found to be 17.8 ± 0.95 GPa, while that of the inner 15.9 ± 0.7 GPa. For the steel base, its value is 1.70 ± 0.07 GPa.

Microhardness is practically constant within both boride layers and the steel base and slightly diminishes (by about 0.2 GPa) with increasing distance in the range 0–300 μm from the inner boride layer.

Layer-Growth Kinetics

After the continuous layers of both borides have formed, their subsequent diffusional growth is due to two partial chemical reactions (Fig. 6)

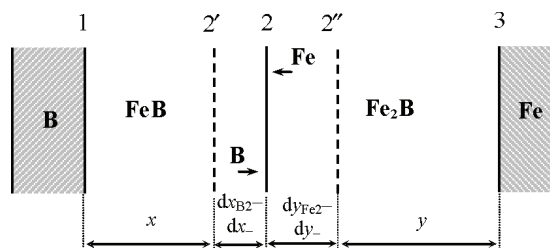


and



Fig. 6. Schematic illustration of the growth process of two boride layers under diffusion-controlled conditions:

both layers thicken at their common interface 2; no reactions take place at interfaces 1 and 3 in view of lack of appropriate diffusing atoms



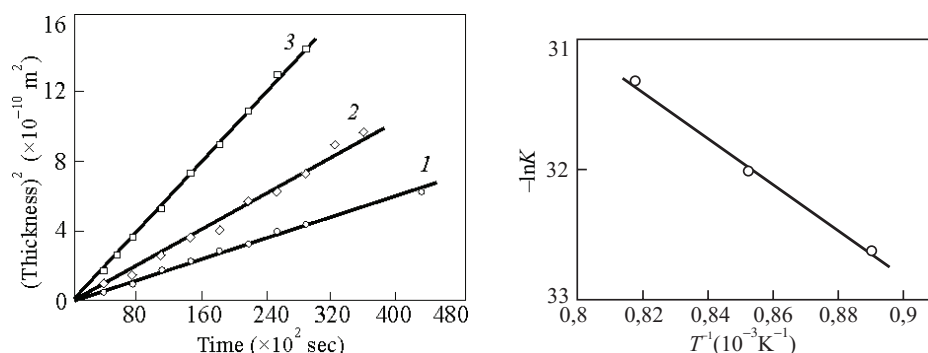


Fig. 7. A plot of the square of the total thickness of both boride layers against time at a temperature of 850 (1), 900 (2), and 950 °C (3)

Fig. 8. The temperature dependence of the growth-rate constant for both boride layers formed at the steel–boron interface

In view of the close similarity of physicochemical properties of FeB and CrB as well as Fe₂B and Cr₂B, the chemical-reaction equations are written only for the FeB and Fe₂B phases.

The diffusional growth kinetics of compound layers is usually treated using parabolic equations of the type

$$x^2 = 2k_1t, \quad (2)$$

where x is the layer thickness, k_1 is the layer growth-rate constant, and t is time [18, 19]. For sufficiently thick layers, such equations produce a quite satisfactory fit to the experimental data, as is the case in the present study (Fig. 7). Since the thickness of the inner boride layer was very irregular, only the data for the total thickness of both layers are presented. The reliable separate treatment for each of the two layers could hardly be carried out.

As seen in Fig. 8, the temperature dependence of the layer growth-rate constant is described in the 850–950 °C range by a relation of the Arrhenius type

$$k_1 = k_{10} \exp(-E/RT), \quad (3)$$

where K stands for any layer growth-rate constant, E is the activation energy, R is the gas constant, and T is the absolute temperature.

The least-squares fit method yields the following equation: $k_1 = 1.72 \cdot 10^{-8} \exp(-137.1 \text{ kJ} \cdot \text{mol}^{-1}/RT)$. From this equation, values of the layer growth-rate constant at intermediate temperatures can readily be evaluated.

Abrasive Wear Resistance of Boride Layers

Boriding the steel tablets for dry abrasive wear resistance tests was carried out at 950 °C for 6 h, producing two boride layers (Fe, Cr)B–(Cr, Fe)B and (Fe,Cr)₂B–(Cr,Fe)₂B of total thickness around 35 μm. Five measurements were carried out on each sample and the average values of the mass loss were found. The dry abrasive wear resistance of borided steel samples proved to be more than 250 times greater than that of the steel base.

Conclusions

Two boride layers are formed at the interface of industrial 25% chromium steel (15X25T) and boron powder at 850–950 °C and reaction times up to 12 h.

The outer layer bordering the boron phase consists of the (Fe, Cr)B and (Cr, Fe)B compounds, while that of the inner layer adjacent to the steel base consists of the (Fe, Cr)₂B and (Cr, Fe)₂B compounds.

The characteristic feature of both layers is a pronounced texture.

Diffusional growth kinetics of the boride layers is close to parabolic.

The dry abrasive wear resistance of borided steel samples is more than 250 times greater than that of the nonborided ones.

В результате термохимической обработки промышленной хромовой стали (15X25T–25% Cr) в порошке аморфного бора в температурном интервале 850–950 °C и времени реакции до 43200 с (12 ч) на границе раздела сталь-бор образуются два боридных слоя. Микроструктура внешнего боридного слоя, граничащего с бором, состоит из удлиненных кристаллов соединений (Fe, Cr)B и (Cr, Fe)B, а микроструктура внутреннего боридного слоя, прилегающего к стальной основе, состоит из удлиненных кристаллов соединений (Fe, Cr)₂B и (Cr, Fe)₂B. Для обоих слоев характерна четкая выраженная текстура. Кинетика их диффузионного роста близка к параболической $x^2 = 2k_1t$, где x — общая толщина обоих слоев (м), k_1 — константа скорости роста слоев ($\text{м}^2 \cdot \text{с}^{-1}$) и t — время (с). Температурная зависимость константы скорости роста боридных слоев на поверхности стали описывается зависимостью Аррениусовского типа $k_1 = 1,72 \cdot 10^{-8} \exp(-137,1 \text{ кДж} \cdot \text{моль}^{-1}/RT)$. Величина микротвердости составляет 17,8 ГПа для внешнего слоя, 15,9 ГПа для внутреннего слоя и 1,70 ГПа для стальной основы. Сухая абразивная износостойкость борированных образцов стали более, чем в 250 раз выше износостойкости неборированных образцов.

Ключевые слова: термохимическая обработка, хромовая сталь (15X25T–25% Cr), порошок аморфного бора, боридные слои, микроструктура, кинетика роста, микротвердость, абразивная износостойкость.

Thermochemical treatment of industrial chromium steel ((15Kh25T–25% Cr)) in amorphous boron powder in the temperature range 850–950 °C and reaction times up to 43200 sec (12 h) results in the formation of two boride layers at the steel–boron interface. The microstructure of the outer layer bordering the boron phase consists of elongated crystals of the (Fe,Cr)B and (Cr,Fe)B compounds, while that of the inner layer adjacent to the steel base consists of elongated crystals of the (Fe,Cr)₂B and (Cr,Fe)₂B compounds. Both layers reveal a pronounced texture. Their diffusional growth kinetics is close to parabolic $x^2 = 2k_1t$, where x is the total thickness of both layers (m), k_1 is the layer growth-rate constant ($\text{m}^2 \cdot \text{sec}^{-1}$), and t is time (sec). The temperature dependence of the growth-rate constant of boride layers on the steel surface is described by a relation of the Arrhenius type $k_1 = 1.72 \cdot 10^{-8} \exp(-137.1 \text{ kJ} \cdot \text{mole}^{-1}/RT)$. Microhardness values are 17.8 GPa for the outer layer, 15.9 GPa for the inner layer, and 1.70 GPa for the steel base. The dry abrasive wear resistance of borided steel samples is more than 250 times greater than that of non-borided ones.

Keywords: thermochemical treatment, chromium steel (15Kh25T–25% Cr), amorphous boron powder, boride layers, microstructure, growth kinetics, microhardness, abrasive wear resistance.

1. Voroshnin L. G. Steel Boriding [in Russian] / L. G. Voroshnin, L. S. Lyakhovich. – Moscow: Metallurgiya, 1978. – 240 p.
2. Voroshnin L. G. Boriding of Industrial Steels and Cast Irons [in Russian]. – Minsk, Belarus, 1981. – 208 p.
3. Sinha A. K. Boriding (boronizing) // Metals Handbook; ed. by A. K. Sinha. – Metals Park, Ohio: ASM International, 1982. – P. 844.
4. Kunst H. Metals, surface treatment // Ullmann's Encyclopedia of Industrial Chemistry / H. Kunst, H. Schroll, R. Luetje et al. – Weinheim: Verlag Chemie, 1991. – Vol. A16. – P. 427.
5. Hansen M. Constitution of Binary Alloys; 2nd ed. – New-York: McGraw-Hill, 1958. – 249 p.

6. *Vol A. E.* Constitution and Properties of Binary Metal Systems [in Russian]. – Moscow: Fizmatgiz, 1962. – Vol. 1. – 679 p.
7. *Okamoto H.* B–Fe (Boron–Iron) // *J. Phase Equilib. Diffusion.* – 2004. – Vol. 25. – P. 297–298.
8. *Bondar A. A.* Boron–chromium–iron // *Landolt-Börnstein*; ed. by G. Effenberg, S. Ilyenko. – Berlin–Heidelberg: Springer, 2007. – Vol. 11D1. – P. 320–343.
9. *Dybkov V. I.* Formation of boride layers at the Fe–10% Cr alloy–boron interface / V. I. Dybkov, W. Lengauer, K. Barmak // *J. Alloys Compd.* – 2005. – Vol. 398. – P. 113–122.
10. *Brandstötter J.* Reaction diffusion in transition metal–boron systems / J. Brandstötter, W. Lengauer // *Ibid.* – 1997. – Vol. 390–396. – P. 390–396.
11. *Mirkin L. I.* Handbook of X-Ray Structure Analysis of Polycrystals [in Russian]. – Moscow: Fizmatgiz, 1961. – 864 p.
12. *Gorelik S. S.* X-Ray and Electron Optical Analyses: Applications [in Russian] / S. S. Gorelik, L. N. Rastorguev, Yu. A. Skakov. – Moscow: Metallurgiya, 1970. – 106 p.
13. *Barinov V. A.* Structure and magnetic properties of the α -FeB phase obtained by mechanical working / V. A. Barinov, G. A. Dorofeev, L. V. Ovechkin et al. // *Phys. Stat. Sol. A.* – 1991. – Vol. 123. – P. 527–534.
14. *Gianoglio C.* Distribution equilibria of iron and nickel in two phase fields of the Fe–Ni–B system / C. Gianoglio and C. Badini // *J. Mater. Sci.* – 1986. – Vol. 21. – P. 4331–4334.
15. *Okada S.* Structural investigation of Cr₂B₃, Cr₃B₄, and CrB by single-crystal diffractometry / S. Okada, T. Atoda, and I. Higashi // *J. Solid State Chem.* – 1987. – Vol. 68. – P. 61–67.
16. *Gianoglio C.* Solid state equilibria in the Cr–Fe–B system at the temperature of 1373 K / C. Gianoglio, G. Pradelli, M. Vallino // *Metall. Sci. Technol.* – 1983. – Vol. 1. – P. 51–57.
17. *Martini C.* Mechanism of thermochemical growth of iron borides on iron / C. Martini, G. Palombarini, and M. Carbucicchio // *J. Mater. Sci.* – 2004. – Vol. 39. – P. 933–937.
18. *Seith W.* Diffusion in Metals [in German]. – Berlin: Springer, 1955.
19. *Hauffe K.* Reactions in and on Solids [in German]. – Berlin: Springer, 1955.

Institute for Problems of Materials Science, Department of Physical Chemistry of Inorganic Materials, Kyiv, Ukraine Submitted 14.06.11